

Imaging meddy finestructure using multichannel seismic reflection data

B. Biescas,¹ V. Sallarès,¹ J. L. Pelegrí,² F. Machín,² R. Carbonell,³ G. Buffett,³
J. J. Dañobeitia,¹ and A. Calahorrano²

Received 13 March 2008; revised 16 April 2008; accepted 2 May 2008; published 14 June 2008.

[1] This work illustrates the great potential of multichannel seismic reflection data to extract information from the finestructure of meddies with exceptional lateral resolution (10–15 m). We present seismic images of three meddies acquired in the Gulf of Cadiz (SW Iberian Peninsula), which consist of concentric reflectors forming oval shapes that sharply contrast with the background oceanic structure. The seismic images reveal the presence of different regions within the meddies that are consistent with those observed in historical temperature (T) and salinity (S) data. The core region, characterized by smooth T and S variations, is weakly reflective. The double-diffusive upper and lower boundaries and the lateral-interleaving outer edges, characterized by stronger T and S contrasts, display strong reflectivity bands. These new observations clearly show differences between layers developed at the upper and lower boundaries that can contribute to the knowledge of mixing processes and layering formation in oceans. **Citation:** Biescas, B., V. Sallarès, J. L. Pelegrí, F. Machín, R. Carbonell, G. Buffett, J. J. Dañobeitia, and A. Calahorrano (2008), Imaging meddy finestructure using multichannel seismic reflection data, *Geophys. Res. Lett.*, 35, L11609, doi:10.1029/2008GL033971.

1. Introduction

[2] The warm and salty Mediterranean water spills over the Strait of Gibraltar (Figure 1), sinks and flows westwards along the continental slope of the South Iberian margin, forming the so-called Mediterranean Undercurrent (MU) [Ambar *et al.*, 2002]. During its journey along the margin, the MU experiences abrupt topographic changes like major canyons, causing boluses of Mediterranean water to separate from the MU in the form of ~40–100 km wide, ~1 km thick, vertically extending between ~500 and 1500 m depth, coherent clockwise-rotating lenses called meddies [Richardson *et al.*, 2000]. Generally, meddies translate first to the west and then drift southwestwards near Cape St Vincent towards the Canary basin with translation speeds of a few cm/s and anti-cyclonic rotation periods of 4 to 6 days [Richardson *et al.*, 2000]. During the life of a lens, the Mediterranean water slowly mixes with the surrounding Atlantic water and salt anomalies progressively weaken until the meddy dissipates. Meddies may last for about 2 years and cover distances up to one thousand km [Armi *et al.*, 1989; Richardson *et al.*, 1989, 2000].

¹Unitat de Tecnologia Marina CSIC, Barcelona, Spain.

²Institut de Ciències del Mar CSIC, Barcelona, Spain.

³Institut de Ciències de la Terra Jaume Almera CSIC, Barcelona, Spain.

[3] The existing information on the internal structure and dynamic processes taking place within meddies is mainly based on data acquired using classical oceanographic instrumentation with a lateral resolution of $\mathcal{O}(1\text{ km})$. In their pioneering work, Holbrook *et al.* [2003] showed that marine multichannel seismic (MCS) data, designed and used to obtain structural images of the Earth's subsurface, also display coherent reflections from within the water layer. Thanks to signal redundancy provided by the multiple fold of a single reflector point, MCS systems enhance coherent signals over noise, resulting in clear acoustic images of the oceanic thermohaline structure with a lateral resolution of $\mathcal{O}(10\text{ m})$. Based on Holbrook and coworkers' images, as well as on his own results, Ruddick [2003] pointed at the potential of MCS data to image the finestructure that is likely to develop at the bounds of meddies owing to double-diffusion vertical mixing (upper and lower bounds) and interleaving (lateral bounds).

[4] In this work we confirm the potential of MCS data to locate meddies and to image their internal structure with great detail by showing three spectacular MCS images of complete meddies that reveal a number of significant features, including the distribution of finestructure with lateral and vertical resolution of 10–15 m.

2. Data Acquisition and Processing

[5] The MCS data used in this work were acquired in the Gulf of Cadiz in the framework of the Iberian-Atlantic Margin (IAM) survey [Torné *et al.*, 1995] that took place in August–September 1993 (Figure 1a). IAM data were recorded using a 4800 m long HSSQ/GX600 analogue streamer with 192, 25 m-spaced channels, giving a common depth point (cdp) spacing (i.e., a lateral sampling) of 12.5 m. The seismic source was an airgun array composed of 36 BOLT guns with a total volume of 7524 cu. in. and a peak energy in the frequency band of 20–50 Hz that were fired with a pop interval of 75 m. The theoretical vertical resolution of seismic reflection systems is considered to be a quarter of wavelength [Yilmaz, 2001], although this resolution is rarely achieved since it is affected by factors such as the thickness of the reflecting horizon and the sharpness of the boundary between the media. Therefore the vertical resolution is more realistically on the order of one half of wavelength, i.e., ~15 m for the highest IAM's source frequency.

[6] We fully reprocessed some of the IAM profiles with the aim of obtaining the best possible images of the water column. The processing sequence consisted of the following six steps [Yilmaz, 2001]: (1) Bandpass frequency filter between 5 and 120 Hz and spherical divergence gain

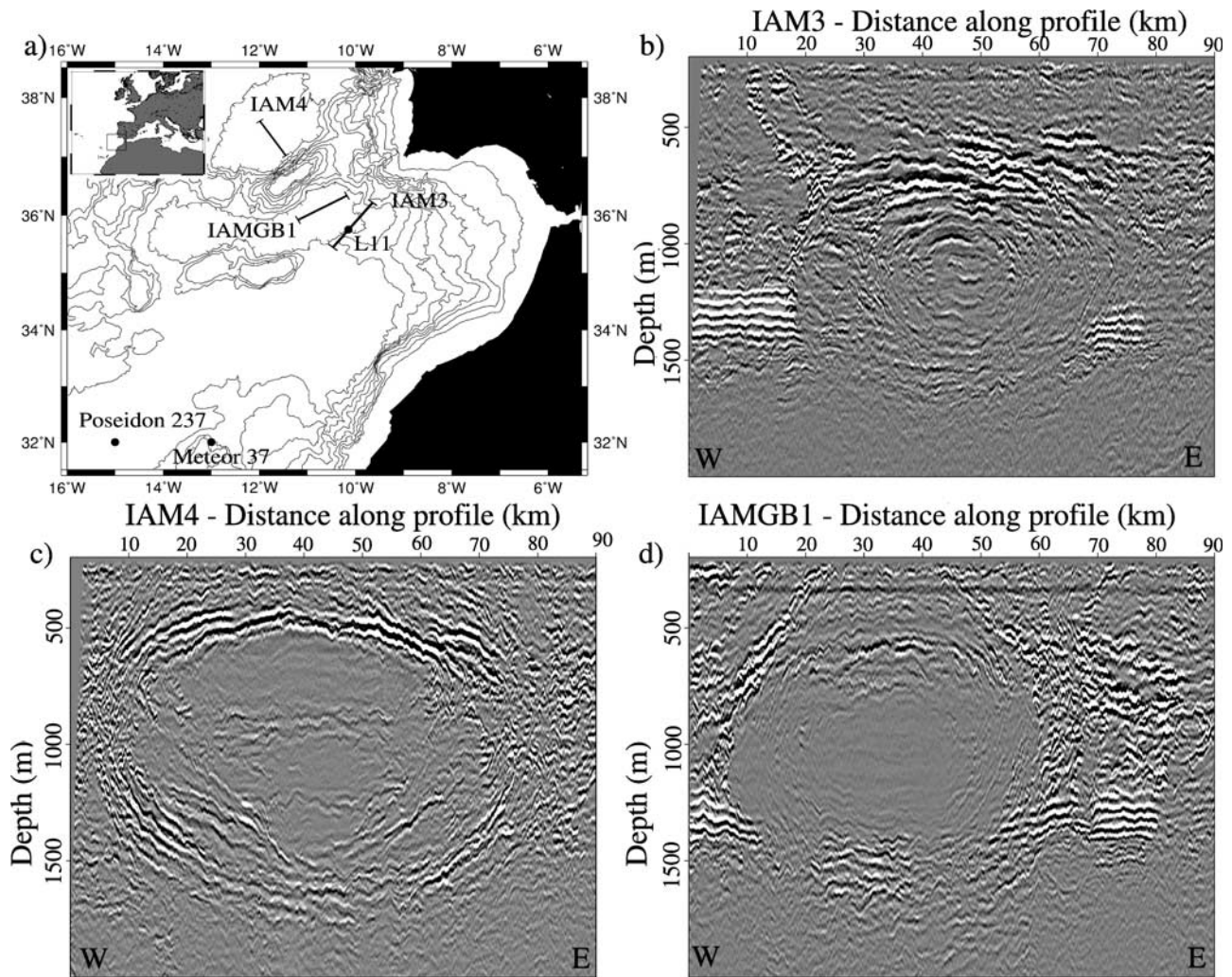


Figure 1. (a) Map showing the geographical location of the study zone. Lines indicate the position of the MCS profiles that were reprocessed in the present work, acquired during the IAM survey in autumn 1993. Black dots correspond to the location of CTD probes acquired in the framework of the CANIGO project during winter 1997 (Meteor 37), spring 1998 (Poseidon 237) and autumn 1997 (L11). MCS images of profiles (b) IAM3 on August 31st, (c) IAM4 on August 29th and (d) IAMGB1 on September 7th.

correction. (2) Median subtraction-filter to remove the direct wave. The direct wave, which travels from source to receiver without being reflected is, by far, the most energetic one and masks shallow-water reflections. It is thus important to eliminate this phase without removing the reflected ones. (3) Velocity analysis. (4) High order normal moveout correction. (5) Stacking of cdp-sorted traces with offsets larger than 600 m to mitigate the direct wave in the near-offset field, where median filtering is less efficient. And (6) Post-stack Kirchhoff time migration.

[7] Seismic data (Figures 1b, 1c, and 1d) contain indirect information on magnitudes of oceanographic interest other than purely morphological. The seismic reflection coefficient, or amplitude ratio of the reflected vs. incident waves, is proportional to the contrast in acoustic impedance (sound speed times density) between two contacting media (thicker than ~ 15 m in our case) [Sheriff and Geldart, 1982]. Insofar as density and velocity are primarily a function of temperature and salinity [Munk et al., 2003], seismic reflectors and their amplitudes must be coherent with, and provide infor-

mation on, the finestructure in terms of salinity and temperature contrasts [Nandi et al., 2004]. With the purpose of exploring the correspondences between seismic and oceanographic data, we compiled a number of existing conductivity-temperature-depth (CTD) profiles that sampled meddies (Figure 1a). These CTDs were acquired during the Canary Islands, Azores and Gibraltar Observations (CANIGO) project [Parrilla et al., 2002], and the meddies are thus other than the seismically imaged ones.

3. Results: Imaging Meddy Finestructure

[8] Three out of ten IAM MCS profiles reprocessed in the course of this work show prominent meddy-like features, i.e., large oval-shaped structures outlined by a series of concentric seismic reflectors with lateral diameters of some 50–80 km and vertical thickness of 1000–1500 m, centered at a depth of ~ 1000 m, which sharply contrast with the background acoustic ocean's structure (Figure 1). Table 1 displays some properties of the upper and lower reflectors,

Table 1. Number of Digitized Reflectors, Mean Length, Maximum Length, Maximum and Minimum Amplitudes of Acoustic Reflectors in the Upper and Lower Boundaries of Meddies IAM3, IAM4 and the Lower Boundary of IAMGB1

| Meddy | Num. Digitized Reflectors | Mean Length (km) | Max. Length (km) | Max. Amp. Counts | Mean Amp. Counts |
|---------------------|---------------------------|------------------|------------------|------------------|------------------|
| IAM3 [500–1000]m | 18 | 8.8 | 19 | 20 | 1.5 |
| IAM3 [1400–1700]m | 30 | 2 | 5.1 | 4.5 | 0.5 |
| IAM4 [400–600]m | 10 | 15.1 | 32.7 | 20 | 1 |
| IAM4 [1200–1800]m | 76 | 2.9 | 10.6 | 5.5 | 0.5 |
| IAMGB1 [1200–1800]m | 60 | 2.6 | 7.1 | 7 | 0.5 |

such as their maximum and mean lengths and seismic signal amplitudes.

[9] The meddy found along profile IAM3 (Figure 1b) is the smallest. Considering dimensions based on the concentric seismic reflectors, this meddy is ~ 50 km wide and spreads between 700 m and 1600 m. It is noteworthy that IAM3 is the only one of the three meddies in which seismic reflectors are observed throughout the whole structure, from the boundary zone to the central region. The reflective bands that delineate the upper boundary show maximum length of ~ 19 km and vertical separations between single reflectors of ~ 40 –60 m, while the lower ones show shorter lateral lengths (~ 5 km) and more variable vertical separations (20–50 m). The meddy seismic imaged in the IAM4 profile (Figure 1c) has a diameter of 80 km and extends from 400 m to 1800 m depth. The concentric reflectors outlining the meddy are located on the perimeter and do not extend toward the core region. The center of the meddy shows a band of horizontal reflectors at about 900 m depth, which appear to separate two nearly acoustically invisible cores. The reflective layers on the upper edge spread over a ~ 100 m thick band, with maximum length of ~ 32 km and vertical separations of about 40–50 m between single reflectors, while in the lower edge the high-reflectivity band is ~ 400 m thick, reflectors have much shorter lateral lengths and more variable vertical separation (20–50 m). Finally, the seismic image of the meddy in the IAMGB1 line (Figure 1d) has a diameter of ~ 60 km and a vertical thickness of 1500 m. The geometry of the lateral layers suggests that the top of the meddy could be located in the shallowest ~ 100 m depth, where we do not have good quality acoustic data because of the direct wave distortion. However, there is no observation of a meddy T and S anomaly extending to the surface, thus there might be another process that accounts for these lateral and shallow reflections. Some strong reflectors can be observed at ~ 600 m depth; nevertheless, it is difficult to determine if they distinguish two different cores or they actually form the upper boundary of a single core that has a dome-shaped structure on top. The lower boundary is ~ 400 m thick and shows relatively short reflective layers with vertical separation of ~ 20 –40 m. The flat line observed at ~ 400 m depth along all the seismic image corresponds to the direct wave, which could not be totally removed by the median filter.

4. Discussion

[10] The presence of differentiated, well-defined, temporally-evolving regions within meddies was first suggested based on data acquired during the repeated sampling of a meddy called Sharon that was tracked for two years in the eastern North Atlantic subtropical gyre [Armi *et al.*, 1989; Richardson *et al.*, 1989; Ruddick, 1992; Hebert *et al.*,

1999]. Sharon was characterized by a single central core with very weak spatial thermohaline gradients, that was surrounded by well-developed finestructure. The structure above and below the core was suggested to be caused by double-diffusive vertical mixing while the layering on its lateral bounds was attributed to double-diffusive intrusions.

[11] The seismic snapshots of meddies IAM4 and IAMGB1 are in relative agreement with the oceanographic description in what concerns the core region, since they clearly show a central region with very weak reflectivity. Meddy IAM4 has two cores that are located at the two levels of the Mediterranean outflow water (800 and 1200 m) [Ambar *et al.*, 2002]. Both cores are separated by the reflection layers visible at about 950 m, the shallow one being dome-shaped and the deep core having an inverted dome-shaped. Meddy IAMGB1 could have a single or double-core, actually indistinguishable in the seismic image because of the lateral reflectors extend towards the surface. In contrast, meddy IAM3 does not show an acoustically transparent core. It appears rather to have quite well developed finestructure that reaches almost to its center. This feature, together with the relatively small apparent radius of meddy IAM3 (~ 25 km), suggests two possible explanations: that the seismic snapshot may have crossed it quite away from its center, at a position in the outer intrusively-mixed region, or that it is an old meddy so that lateral intrusions had worked their way into its center.

[12] Seismic data (Figure 1 and Table 1) reveal that both the upper and lower boundary layers have strong reflectivity, consistent with the existence of finestructure, but suggest significant differences between these regions. The upper boundary zone is relatively thin (~ 100 –200 m), has a few layers that show high lateral coherence and high reflection amplitudes. The vertical separation between layers are slightly longer (~ 40 –60 m) than those observed in the lower boundary. The lower boundary is relatively thick (~ 300 –400 m) and has many, relatively short, layers with a vertical spacing of ~ 20 –50 m and low reflection amplitudes.

[13] Besides MCS data, we have also analyzed available historical oceanographic CTD data that sampled three meddies during different surveys carried out in the Gulf of Cadiz and Canary Basin. To allow qualitative comparison, Figure 2 displays the oceanographic data calculated from the CTD L11 station and the seismic reflections recorded through the center of meddy IAM3. Temperature and salinity data (Figures 2a and 2b) display the main regions of the meddy, which can also be recognized from the acoustic reflectors (Figure 2e). The CTD-L11 data show a double-core meddy with an upper core between 800 and 1000 m depth and a lower core between 1000 and 1300 m depth. Within the core regions, where temperature and

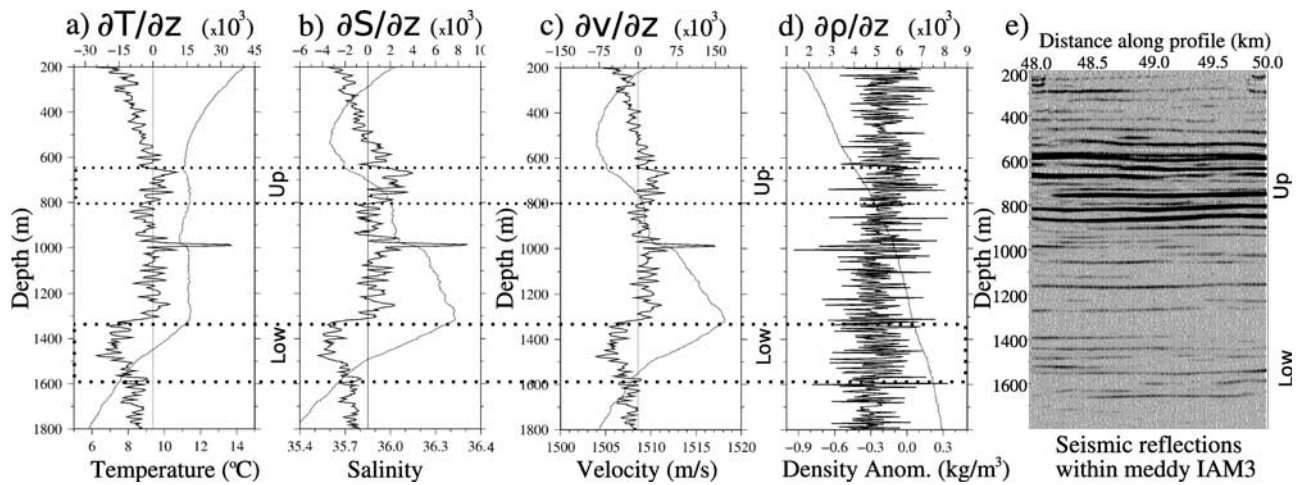


Figure 2. The 5-m smoothed profiles of (a) temperature (dotted line) and temperature gradient (black line), (b) salinity (dotted line) and salinity gradient (black line), (c) sound speed (dotted line) and sound speed gradient (black line), and (d) density anomaly (here defined as in situ density minus density of standard meddy water, i.e., $\rho(S, T, p) - \rho(S = 35, T = 10^\circ\text{C}, p)$) (dotted line) and density gradient (black line) obtained from the CTD probes through the meddy observed during L11. (e) Seismic reflections recorded through the center of meddy IAM3. Geographical locations of the data are shown in Figure 1a.

salinity reach maximum values ($T > 15^\circ\text{C}$, $S > 36.4$), gradients become weaker, while in the intrusive regions, where acoustic reflectors become stronger, temperature and salinity gradients reach maximum values. Since acoustic impedance of a media is the product of sound speed and density, we have calculated these magnitudes from CTD data using *Fofonoff and Millard* [1983] and *Millero et al.* [1980] algorithms. The differences between the upper and lower meddy reflectors are consistent with observed differences in the sound speed profiles (Figure 2c). The relatively thin (~ 150 m) upper boundary is characterized as having

just a few large peaks in the sound speed gradient ($> \pm 50 \cdot 10^3 \text{ s}^{-1}$), with large vertical spacing between peaks (~ 30 – 40 m). The relatively thick lower boundary (~ 300 m), on the contrary, has many more large sound speed gradient peaks, and the vertical spacing between peaks is small (~ 10 – 30 m). Velocity gradients dominate the acoustic signal since $\rho \partial v / \partial z$ is typically one order of magnitude greater than $v \partial \rho / \partial z$. However, results show that density gradients (Figure 2d) are slightly higher on the core boundaries, where acoustic signal is stronger.

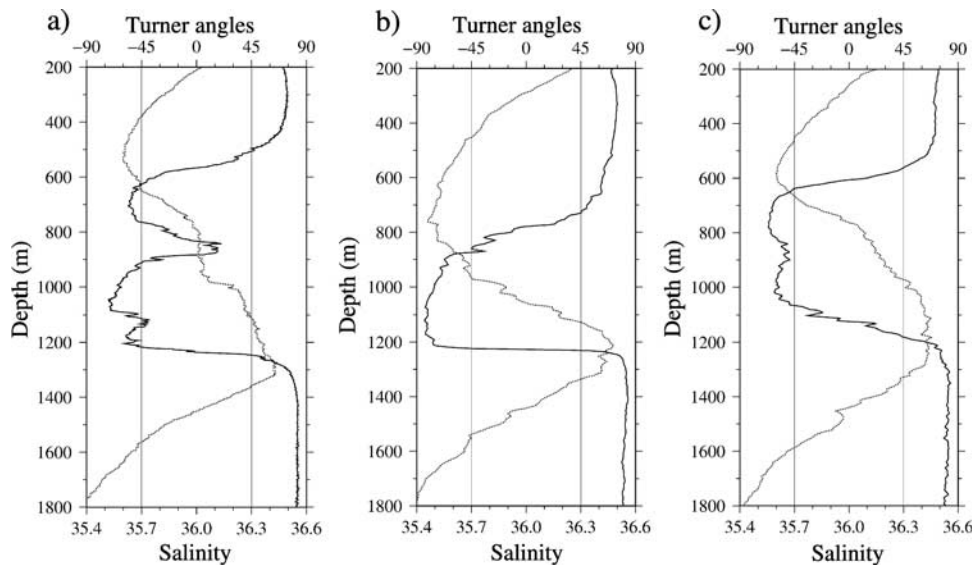


Figure 3. Turner angles (black lines) and salinity profiles (grey lines) as obtained from the CTD through the meddies observed during (a) L11, (b) Meteor 37, and (c) Poseidon 237. Turner angles are practical indicators that differentiate regions prone to diffusive convection ($-90^\circ < Tu < -45^\circ$) and salt finger instability ($45^\circ < Tu < 90^\circ$) from stable regions ($|Tu| < 45^\circ$). Turner angles were calculated, after smoothing the data with a 50 m running vertical window, using the method proposed by *Ruddick* [1983]. Geographical locations are shown in Figure 1a.

[14] One likely explanation for the observed differences between the upper and lower intrusive regions is the different dynamical processes that control their formation and development. Double-diffusive fluxes, based on the molecular heat diffusion being much greater than molecular salt diffusion, can break relatively smooth thermohaline gradients into steps and layers [Ruddick and Gargett, 2003]. Ruddick [1992] actually suggested that the upper boundary of meddies is dominated by diffusive convection, whereas the lower one is prone to salt fingering. Turner angles (Tu) [Ruddick, 1983] calculated from the CTD data, indeed show that the upper and lower bounds of all three CANIGO meddies are prone to diffusive-convection and salt-fingers, respectively, while their core regions are double-diffusively stable (Figures 3a, 3b, and 3c). The seismic images provide thus a very valuable two-dimensional view of the patterns that result from different regimes and should contribute to improve both phenomenological and numerical models of mixing and layering formation in geophysical fluids.

5. Conclusions

[15] Seismic oceanography is becoming a useful tool to investigate the internal structure of the water column. Multichannel seismic (MCS) data presented in this work corroborate the great potential of this method for studying oceanic processes. Focusing on meddy research, we may now affirm that the MCS method allows to detect these rotating salty lenses, while giving information on their dimensions, as well as the detailed vertical and lateral distribution and characteristics of finestructure. The main regions within a meddy, detected by classical oceanographic instrumentation are clearly observed in the seismic snapshots: (1) the upper boundary zone, characterized by the presence of a few, strong, laterally continuous reflectors, (2) the lower boundary zone, with more numerous shorter and 3–4 times weaker reflectors distributed into a thicker region, and (3) a very weakly reflective central core region. Our results show that powerful 36 BOLT guns array with a total volume of 7524 cu and low frequency (20–50 Hz) sources, such as those used in deep seismic surveys (DSS), are well-suited to image the oceanic finestructure. The unprecedented horizontal resolution of MCS data, two orders of magnitude better than typical oceanographic data, reveal lateral coherence characteristics of the finestructure that should considerably contribute to improving the models of ocean dynamic processes.

[16] **Acknowledgments.** This work was supported by the GEOCEAN Intramural Project (200530f081) funded by the Consejo Superior de Investigaciones Científicas. We are deeply grateful to Dirk Klaeschen for

his help on the seismic processing. We also acknowledge the support of the GO Research Group (NEST-2003-1- Adventure FP6-015603) and the constructive suggestions of two anonymous reviewers.

References

- Ambar, I., N. Serra, M. Brogueira, G. Cabeçadas, F. Abrantes, P. Freitas, C. Gonçalves, and N. González (2002), Physical, chemical and sedimentological aspects of the Mediterranean outflow off Iberia, *Deep Sea Res., Part II*, *49*, 4163–4177.
- Armi, L., D. Herbert, N. Oakey, J. Price, P. Richardson, H. Rossby, and B. Ruddick (1989), Two years in the life of a Mediterranean salt lens, *J. Phys. Oceanogr.*, *19*, 354–370.
- Fofonoff, P., and R. Millard (1983), Algorithms for computation of fundamental properties of seawater, *UNESCO Tech. Pap. Mar.*, *44*.
- Hebert, D., N. Oakey, and B. Ruddick (1999), Evolution of a Mediterranean salt lens: Scalar properties, *J. Phys. Oceanogr.*, *20*, 1468–1483.
- Holbrook, W., P. Páramo, S. Pearse, and W. Schmitt (2003), Thermohaline fine structure in an oceanographic front from seismic reflection profiling, *Science*, *301*, 821–824.
- Millero, F., C. Chen, A. Bradshaw, and K. Schleicher (1980), A new high pressure equation of state for seawater, *Deep Sea Res., Part A*, *27*, 255–264.
- Munk, W., P. Worcester, and C. Wunsch (2003), *Ocean Acoustic Tomography, Cambridge Monogr. Mech.*, vol. 56, 570 pp., Cambridge Univ. Press, Cambridge, U. K.
- Nandi, P., W. Holbrook, S. Pearse, P. Páramo, and R. Schmitt (2004), Seismic reflection imaging of water mass boundaries in the Norwegian Sea, *Geophys. Res. Lett.*, *31*, L23311, doi:10.1029/2004GL021325.
- Parrilla, G., S. Neuer, P. Le Traon, and E. Fernández-Suárez (2002), Canary Islands Azores Gibraltar Observations (CANIGO): Studies in the northern Canary Islands basin, *Deep Sea Res. Part II*, *49*, 3409–3413.
- Richardson, P., D. Walsh, L. Armi, M. Schröder, and J. Price (1989), Tracking three meddies with SOFAR floats, *J. Phys. Oceanogr.*, *19*, 371–383.
- Richardson, P., A. Bower, and W. Zenk (2000), A census of meddies tracked by floats, *Prog. Oceanogr.*, *45*, 209–250.
- Ruddick, B. (1983), A practical indicator of the stability of the water column to double-diffusive activity, *Deep Sea Res., Part A*, *30*, 1105–1107.
- Ruddick, B. (1992), Intrusive mixing in a Mediterranean salt lens: Intrusion slopes and dynamical mechanisms, *J. Phys. Oceanogr.*, *22*, 1274–1285.
- Ruddick, B. (2003), Sounding out ocean fine structure, *Science*, *301*, 772–777.
- Ruddick, B., and A. Gargett (2003), Oceanic double-infusion: Introduction, *Prog. Oceanogr.*, *56*, 381–393.
- Sheriff, R., and L. Geldart (1982), *Exploration Seismology: History, Theory and Data Acquisition*, 253 pp., Cambridge Univ. Press, Cambridge, U. K.
- Torné, M., M. Fernández, J. Carbonell, and E. Banda (1995), Lithospheric transition from continental to oceanic in the West Iberia Atlantic Margin, in *Rifted Ocean-Continent Boundaries, NATO ASI Ser. C*, vol. 463, edited by E. Banda, M. Torné, and M. Talwani, pp. 247–263, Springer, New York.
- Yilmaz, O. (2001), *Seismic Data Analysis: Processing, Inversion, and Interpretation of Seismic Data*, vol. II, *Invest. Geophys.*, vol. 10, 2nd ed., 2027 pp., Soc. Explor. Geophys., Tulsa, Okla.

B. Biescas, J. J. Dañobeitia, and V. Sallarrès, Unitat de Tecnologia Marina, Passeig Marítim de la Barceloneta 37-49, E-08003 Barcelona, Spain. (biescas@cmima.csic.es)

G. Buffett and R. Carbonell, Institut de Ciències de la Terra Jaume Almera CSIC, Lluís Sole Sabaris s/n, E-08028 Barcelona, Spain.

A. Calahorrano, F. Machín, and J. L. Pelegrí, Institut de Ciències del Mar CSIC, Passeig Marítim de la Barceloneta 37-49, E-08003 Barcelona, Spain.